PHILOSOPHICAL TRANSACTIONS OF THE ROYAL SOCIETY B

Phil. Trans. R. Soc. B (2009) **364**, 2589–2602
doi:10.1098/rstb.2009.0068

Serotonin targets inhibitory synapses to induce modulation of network functions

Till Manzke[1,2,3], Mathias Dutschmann[1,4], Gerald Schlaf[5], Michael Mörschel[1,4], Uwe R. Koch[1], Evgeni Ponimaskin[1,3], Olivier Bidon[1], Peter M. Lalley[6] and Diethelm W. Richter[1,3,*]

[1]*Department of Neuro- and Sensory Physiology, and* [2]*Department of Child and Adolescent Psychiatry, University of Göttingen, 37073 Göttingen, Germany*
[3]*DFG Research Center Molecular Physiology of the Brain (CMPB), 37073 Göttingen, Germany*
[4]*Bernstein Center for Computational Neuroscience, 37073 Göttingen, Germany*
[5]*Department of Medical Immunology, University of Halle-Wittenberg, 06097 Halle, Germany*
[6]*Department of Physiology, University of Wisconsin, Madison, WI 53706, USA*

The cellular effects of serotonin (5-HT), a neuromodulator with widespread influences in the central nervous system, have been investigated. Despite detailed knowledge about the molecular biology of cellular signalling, it is not possible to anticipate the responses of neuronal networks to a global action of 5-HT. Heterogeneous expression of various subtypes of serotonin receptors (5-HTR) in a variety of neurons differently equipped with cell-specific transmitter receptors and ion channel assemblies can provoke diverse cellular reactions resulting in various forms of network adjustment and, hence, motor behaviour.

Using the respiratory network as a model for reciprocal synaptic inhibition, we demonstrate that 5-HT_{1A}R modulation primarily affects inhibition through glycinergic synapses. Potentiation of glycinergic inhibition of both excitatory and inhibitory neurons induces a functional reorganization of the network leading to a characteristic change of motor output. The changes in network operation are robust and help to overcome opiate-induced respiratory depression. Hence, 5-HT_{1A}R activation stabilizes the rhythmicity of breathing during opiate medication of pain.

Keywords: glycinergic synapses; serotonin modulation; network operation; disinhibition; rescue breathing

1. INTRODUCTION

Despite detailed knowledge about the molecular processes controlling G protein-coupled receptor (GPCR)-induced modulation of neuronal excitability, we cannot predict the responses of neuronal networks to a global release of neuromodulators. This is due to a diversity of neurons that express cell-specific patterns of GPCRs targeting different membrane conductances, which induce distinct operations of the network. Even more difficult to predict is the endogenous capacity of neuronal networks to adapt to variable conditions while preserving or adjusting elementary processes, such as rhythmic burst generation, activity synchronization and pattern formation. To study such integrated processes of network modulation, it is necessary to know the principles of network architecture, identify cell-specific transmitter receptor/ion channel expression profiles and develop appropriate pharmacological tools to dissect GPCR-specific responses. In such studies of integrated network physiology, the respiratory network is a suitable model system, because it produces an ongoing oscillatory activity and a highly integrated synaptic drive that generates augmenting burst activity. Eupnoeic breathing movements also depend on the network to accurately shape firing patterns and precisely control burst termination and phase transitions (Richter & Spyer 2001). All these processes are effectively adjusted by serotonergic neurons of the Raphé nuclei, which exhibit ongoing discharges (Ballantyne *et al.* 2004) to continuously release serotonin (5-HT; Richter *et al.* 1999).

Most serotonin receptors (5-HTRs) are GPCRs operating through signalling pathways that are shared targets of other transmitters, e.g. noradrenaline, dopamine and opiates. All these GPCRs are abundantly expressed in the pre-Bötzinger complex (pre-BötC; Gray *et al.* 1999; Manzke *et al.* 2003; Viemari & Ramirez 2006), which is an essential part of the respiratory rhythm generator in the medullary brainstem of mammals (Smith *et al.* 1991; Pierrefiche *et al.* 1998; Tan *et al.* 2008). Signalling via most of these GPCRs converges at the shared molecular target adenylyl cyclase (AC), which regulates the formation of cellular cyclic adenosine 5′,3′-monophosphate (cAMP). This has inspired several investigations of the mechanisms of the dynamic adjustment of respiratory network function through regulation of intracellular cAMP levels (Ballanyi *et al.* 1997; Lalley *et al.* 1997; Richter *et al.* 1999; Bocchiaro & Feldman 2004).

*Author for correspondence (d.richter@gwdg.de).

One contribution of 17 to a Discussion Meeting Issue ‘Brainstem neural networks vital for life’.

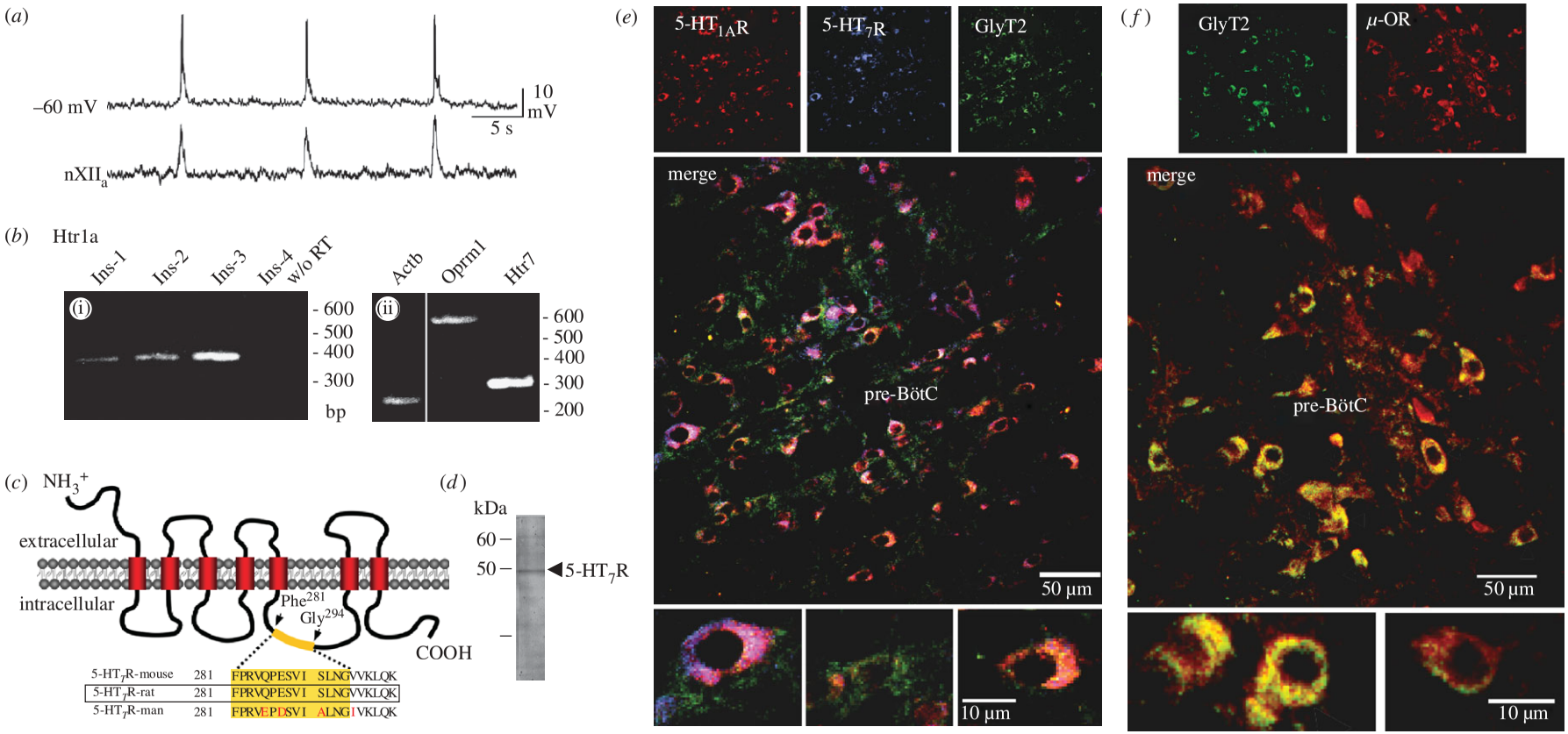

Figure 1. Expression patterns of 5-HT$_{1A}$R, 5-HT$_7$R and GlyT2 in the pre-BötC of rat. (*a*) Whole cell recording in current-clamp mode from an identified respiratory pre-BötC neuron discharging in synchrony with integrated hypoglossal nerve (XIIa) activity (lower trace). The cytosol of this cell was used for single-cell RT–PCR analysis. (*b*) Single-cell RT–PCR analysis of inspiratory neurons. (i) Agarose gel electrophoresis carried out for RT–PCR product amplified from four identified inspiratory neurons (Ins-1–4) with specific primers for Htr1a (5-HT$_{1A}$R). A control reaction without reverse transcription (w/o RT) is shown in the last lane. (ii) RT–PCR products from inspiratory neuron 3 amplified with specific primers for Actb (β-actin), Oprm1 (μ-OR) and Htr7 (5-HT$_7$R). (*c*) A novel monoclonal antibody against 5-HT$_7$R was produced by selecting part of the rat 5-HT$_7$R TM5-TM6 intracellular loop (Phe^{281}–Gly^{294}) for immunization. The epitope is 100 per cent conserved in mouse and rat, and mismatches in the human 5-HT$_7$R sequence are indicated by red lettering. (*d*) The specific signal of approximately 48 kDa in the immunoblot corresponds with the predicted molecular mass of 5-HT$_7$R. (*e*) Triple labelling with the guinea pig anti-5-HT$_{1A}$R antibody (Cy3, red), hamster anti-5-HT$_7$R antibody (Cy5, blue) and rabbit anti-GlyT2 antibody (Cy2, green). The data reveal a predominant expression of 5-HT$_{1A}$R and 5-HT$_7$R in GlyT2-positive inhibitory neurons. (*f*) Double labelling of pre-BötC neurons with the rabbit anti-GlyT2 antibody (Cy2, green) and the guinea pig μ-OR antibody (Cy3, red) revealing abundant expression of μ-OR expression in glycinergic neurons. In a recent study on the reduced brainstem slice preparation (Winter *et al.* 2009), a 20 per cent population of these GlyT2-eGFP-labelled neurons revealed spontaneous respiratory activity.

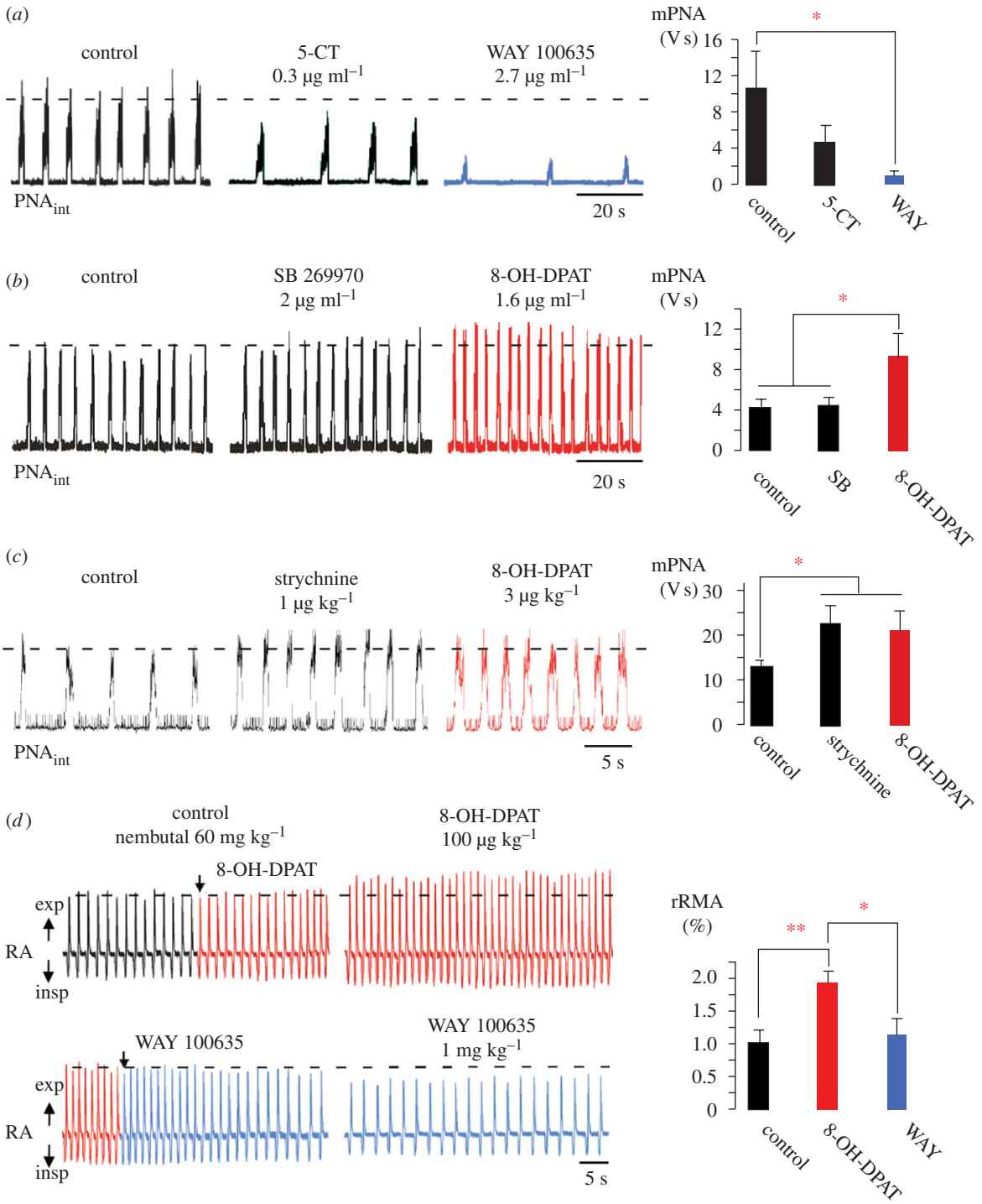

Figure 2. Respiratory network responses to systemic 5-HT_{1A}R and 5-HT_7R ligand applications of *in situ* rats. (*a–c*) Action of 5-HT_{1A}R and 5-HT_7R ligands in the perfused brainstem–spinal cord preparation. (*a*) Application of the 5-HT_7R agonist 5-CT (0.3 µg ml^{-1}) depressed PNA and subsequent application of the 5-HT_{1A}R-antagonist WAY 100635 (2.7 µg ml^{-1}) exacerbated this effect. These data reveal constitutive 5-HT_{1A}R activity under normal conditions. (*b*) Blockade of 5-HT_7Rs by SB 269970 (2.0 µg ml^{-1}) did not change PNA. Subsequent administration of 8-OH-DPAT (1.6 µg ml^{-1}) increased PNA by augmenting both the amplitude and frequency of PNA. (*c*) The effect of 8-OH-DPAT is absent when glycine receptors are blocked with strychnine (1.0 µg ml^{-1}). (*d*) Intravenous administration of 8-OH-DPAT (100 µg kg^{-1}) to anaesthetized rats *in vivo* increased rRMA (red trace). This effect was mainly due to an increase in breathing frequency (RA, respiratory activity; exp, expiration; insp, inspiration). A final injection of the 5-HT_{1A}R antagonist WAY 100635 (1 mg kg^{-1}) blocked these effects, and rRMA returned to below baseline levels (blue trace). Statistical analysis is denoted in the panels on the right side with asterisks indicating significance (*$p < 0.05$; **$p < 0.01$).

An unanswered key question of clinical significance concerns the consequences of convergent signalling via serotonin receptors (5-HTRs) and μ-opioid receptors (μ-ORs). The latter are well-known pharmacological targets for anaesthesia and the treatment of pain. Clinically useful μ-OR agonists, however, depress central respiratory activity, causing cessation of rhythmic breathing movements (Mellen *et al.* 2003; Lalley 2006). An averting medical approach against opioid-induced apnoea is possible with 5-HT_4R agonists that re-activate cellular AC (Manzke *et al.* 2003), but such medication is so far not useful in men because

5-HT_4R agonists that permeate through the blood–brain barrier are not available for clinical practice (Lotsch *et al.* 2005).

In the present experiments, we focused on the convergent signalling of μ-OR and 5-HT_{1A}Rs following the observation that fentanyl-induced depression of breathing is reversed by 5-HT_{1A}R-agonists (Sahibzada *et al.* 2000). This finding is unexpected, because both μ-OR and 5-HT_{1A}R agonists lower cAMP levels and decrease neuronal excitability (Richter *et al.* 1999). A straightforward explanation could be that most 5-HT_{1A}R-agonists such as the applied 8-hydroxy-dipropyl-aminotetralin (8-OH-DPAT) also activate G_s-coupled 5-HT_7Rs (Hedlund *et al.* 2004) that might prevail over the inhibitory $G_{i/o}$–AC pathway, thus restoring intracellular cAMP levels (Hoyer *et al.* 2002). Alternatively, one has to search for more complex changes in network operation if this simplistic explanation is not supported.

2. METHODS

(a) In vivo *cat experiments*

Experiments were performed on 10 adult cats of either sex weighing 2.8–3.8 kg using procedures that have been described in detail in other published studies from this laboratory (Lalley *et al.* 1997; Richter *et al.* 1999). Briefly, cats were anaesthetized with IV pentobarbital sodium in doses sufficient to produce deep surgical anaesthesia. The initial dose was 40 mg kg^{-1} intraperitoneally, followed by supplemental maintenance doses of 4–8 mg kg^{-1} IV, as required. Animals were given atropine methyl nitrate (0.2 mg kg^{-1} intraperitoneally) to minimize airway fluid secretion. Surgical procedures included insertion of a catheter in a femoral artery to monitor blood pressure, and placement of catheters in both femoral veins to administer drugs. Temperature was measured rectally and maintained at 36–38°C by external heating. Immobilization was produced with gallamine triethiodide (4 mg kg^{-1} IV to start and 4–8 mg h^{-1} or more frequently) to assist mechanical stability for intracellular recording. Animals were ventilated with oxygen-enriched (60–70% O_2) room air via a cannula inserted into the trachea. To obtain stable intracellular recordings, a bilateral pneumothorax was performed, and a horseshoe-shaped pressure foot was placed gently on the surface of the dorsal medulla over and near the site of microelectrode insertion. Single-electrode current (SEC) and voltage-clamp (SEVC) recording techniques were performed as described previously (Richter *et al.* 1996). Neurons were impaled with sharp borosilicate glass microelectrodes filled with 2 M K-methylsulphate (DC resistance 50–70 MΩ). Membrane potential was recorded in either balanced-bridge mode, or in discontinuous single-electrode current-clamp mode (SEC-05XL amplifier; npi, Tamm, Germany; bandwidth, DC −10 KHz; switching frequencies in the range of 20–40 kHz). The gain was increased to 100 $\mu A V^{-1}$ by the use of an integrator, without affecting SEVC stability, thus improving the accuracy of the membrane potential control.

The 5-HT_{1A}R agonist 8-OH-DPAT (Sigma-Aldrich) was dissolved in Ringer's solution and administered slowly IV to maintain recording stability. Doses were increased in 5 μg kg^{-1} amounts to a final concentration of 10–50 μg kg^{-1}. The effects of 8-OH-DPAT on respiratory network rhythm were obtained from a population of 4 post-inspiratory and 12 expiratory neurons of the ventrolateral medulla.

(b) In vivo *rat experiments*

Sprague Dawley rats of either sex (250–350 g) were anaesthetized by intraperitoneal injection of pentobarbital (60 mg kg^{-1}). The depth of anaesthesia was tested with a forepaw pinch. In case of reflex responses, an additional dose of pentobarbital was applied (approx. one-tenth of the initial dose). The trachea and right femoral vein were canulated with polyethylene tubing to record respiratory air flow and for drug and fluid injections, respectively. The inspiratory/expiratory airflow was recorded using a MacLab-linked pressure transducer connected to the tracheal tubing. Nociceptive responses were assessed by the tail-flick (TF) response. High-intensity light sufficient to stimulate nociceptors was applied to marked spots (1 cm from the tip of the tail, four spots at an interval of 1 cm), and the TF was quantified by measurement of the latency from 'heat on' to the evoked withdrawal response. The average TF response latency values of three consecutive trials before drug application were used as baseline. To avoid tissue damage, the heating was stopped when the TF latency exceeded 300 per cent of control, concluding TF response abolishment. To prevent central hypoxia, the animals were insufflated with oxygen during the whole experiment and ventilated artificially with room air at low frequency (10–15 breath min^{-1}) after opioid-induced apnoea. Artificial ventilation was immediately stopped after detection of the first signs of spontaneous breathing movements evoked by drug application. At the end of the experiments, all animals were sacrificed using an overdose of pentobarbital that produced irreversible cardiac arrest.

(c) *Perfused brainstem–spinal cord preparation of rat or mouse*

The experiments on the *in vivo*-like *in situ* brainstem–spinal cord preparation were performed on Sprague-Dawley rats (P22–P32) or C57BL mice (P20–P25) as described originally (Paton 1996). For isolating the *in situ* brainstem–spinal cord from higher brain areas, animals were deeply anaesthetized with halothane until apnoea occurred and they were unresponsive to a forepaw pinch. Animals were then decerebrated at the pre-collicular level and cerebellectomized, bisected below the diaphragm and the skin was removed. The upper body was placed in a recording chamber and perfused retrogradely via the thoracic aorta with artificial cerebrospinal fluid (ACSF, containing in mM: 1.25 $MgSO_4$; 1.25 KH_2PO_4; 5 KCl; 125 NaCl; 2.5 $CaCl_2$; 25 $NaHCO_3$; 10 glucose, 70 Ficoll (0.1785 mM)), and gassed with carbogen (5% CO_2/95% O_2; pH 7.35). The perfusate was warmed to 30°C as measured in the skull base, filtered twice and recirculated. Norcuronium-bromide at 0.5 mg 200 ml^{-1} was added for immobilization. The perfusion pressure was set to 45–65 mm Hg. Using a glass suction electrode,

phrenic nerve discharges were recorded as an index of central respiratory rhythm. Drugs were added to the perfusate for specific pharmacological manipulation of 5-HTR and glycine receptors.

(d) *Rhythmic brainstem slice preparation of rat*

Inspiratory neurons in the pre-BötC were recorded in whole-cell mode before harvesting the cytosol for single-cell RT–PCR analysis. Transverse slices (600 μm) were cut from the caudal medulla at the level of the pre-BötC with a vibroslicer (Campden Instruments, Loughborough, UK) and stored in ACSF at room temperature (20–23°C) for at least 30 min before experiments were started. They were then transferred to a recording chamber and kept submerged by nylon fibres for mechanical stabilization. The chamber was mounted on an upright microscope (Axioscope FS; Zeiss, Oberkochen, Germany) and perfused continuously with ACSF (20–23°C) at a flow rate of 5–10 ml min^{-1}. Whole-cell voltage-clamp recordings were obtained with a Multiclamp 700A amplifier (Axon Instruments). Patch electrodes were pulled from borosilicate glass capillaries (Biomedical Instruments, Zülpich, Germany) on a horizontal pipette puller (Zeitz-Instrumente, Munich, Germany) and filled with 'patch solution' containing (in mM): 125 KCl, 1 $CaCl_2$, 2 $MgCl_2$, 4 Na_2ATP, 10 EGTA, 10 HEPES (pH adjusted to 7.2 with KOH). Patch electrodes had DC impedances ranging between 2 and 6 MΩ.

(e) *Pharmacology*

The following pharmaceutical substances were administered in *in vivo* cat experiments: 8-hydroxy-2-(di-*N*-propylamino)-tetralin hydrobromide (8-OH-DPAT; 5-HT_{1A}R agonist; Tocris), buspirone (5-HT_{1A}R agonist; Sigma-Aldrich), WAY 100635 (5-HT_{1A}R antagonist; Sigma-Aldrich), 5-carboxamidotryptamine maleate (5-CT; 5-HT_7R agonist; Tocris), SB 269970 hydrochloride (5-HT_7R antagonist; Tocris), strychnine hydrochloride (glycine receptors antagonist; Sigma-Aldrich), fentanyl citrate salt (μ-OR agonist; Sigma-Aldrich). In the *in vivo* rat experiments, the antagonists WAY 100635, SB 269970 and naloxone were used at a concentration of 1 mg kg^{-1}, whereas 8-OH-DPAT was given at 100 μg kg^{-1} and fentanyl at 10–15 μg kg^{-1}. In the perfused brainstem–spinal cord preparations, 8-OH-DPAT, WAY 100635 and SB 269970 were applied in 5–20 μM concentrations; buspirone, 20–40 μM and 5-CT, 1 μM. Fentanyl was given at a concentration of 10–30 nM and strychnine at 0.4 μM.

(f) *Monoclonal antibody against 5-HT_7R*

Since 5-HT_7Rs show a high amino acid sequence identity in mouse, rat and man, we used Syrian hamsters (Charles River Laboratories), which are evolutionarily more distant from these species, to raise monoclonal 5-HT_7R antibodies. Five Syrian hamsters were immunized with a 14mer peptide derived from the TM5–TM6 intracellular loop of the rat 5-HT_7R (NH_2-FPRVQPESVISLNG-COOH; National Center for Biotechnology Information, http://www.ncbi.nlm.nih.gov/, Accession No.: NP_075227). For immunization purposes, peptides were coupled to keyhole limpet haemocyanin (KLH) using 4-(*N*-maleimido-methyl)-cyclohexane-1-carboxylic acid *N*-hydroxy-succinimide ester. Syrian hamsters were injected subcutaneously with 150 μg KLH-coupled peptide in TiterMax Gold (Sigma, Deisenhofen, Germany) six times over a 28-day interval, followed by two intraperitoneal injections over a 3-day interval of 100 μg antigen. Three days after the last injection, the spleen was removed. The fusion of hamster spleen cells with P3X63Ag8.6.5.3 mouse myeloma cells was performed using polyethylene glycol (PEG4000; Sigma) according to standard protocols. First screenings of mouse-hamster heterohybridoma supernatants to identify peptide-binding antibodies were performed by enzyme-linked immunosorbent assay (ELISA) with solid phase-coated peptide. After isotype characterization using sandwich-ELISA procedure (clone 5HTR7/220; immunoglobulin class: IgG, light chains: λ-type), the antibodies were purified on a protein A-sepharose column with the 'high-salt' method according to standard protocols. The efficiency of purification was tested by Coomassie blue staining of SDS–PAGE gels containing the separated IgG molecules. Under reducing conditions, only the heavy (55 kDa) and light chains (25 kDa) of the IgG molecules were detected.

SDS–PAGE and subsequent immunoblot analysis were performed according to standard protocols. In brief, 150 μg total protein from membrane fractions of Triton X-114-extracted brainstem lysates was boiled in SDS sample buffer under reducing conditions for 5 min. Proteins were separated using a 12 per cent SDS–PAGE and transferred onto a nitrocellulose membrane by electroblotting, with a constant current of 150 mA for 2 h in a semi-dry transfer chamber. The efficacy of protein transfer was tested with both Ponceau staining of the membrane and Coomassie blue staining of the remaining protein in the gel. The membrane was blocked with 2 per cent (w/v) bovine serum albumin (BSA) for 30 min at room temperature and incubated with 5HTR7/220 antibodies at a concentration of 2 μg ml^{-1} for 2 h at room temperature (RT). The secondary horseradish peroxidase-conjugated goat anti-hamster IgG (Dianova, Hamburg, Germany) was used at a dilution of 1 : 4000 for 2 h at RT. Visualization of the antigen–antibody reaction was achieved with diaminobenzidine (Sigma) and hydrogen peroxide. The colour reaction was terminated with TBS/0.05 per cent (v/v) TWEEN 20. Finally, the membrane was air-dried and photographed.

(g) *Immunohistochemistry*

Juvenile rats (P28–P32) were deeply anaesthetized with isoflurane (1-chloro-2,2,2-trifluoroethyl-difluoromethylether; Abbott, Wiesbaden, Germany). The animals were transcardially perfused with 50 ml 0.9 per cent sodium chloride followed by 200 ml 4 per cent phosphate-buffered formaldehyde. The brainstem and spinal cord were removed and post-

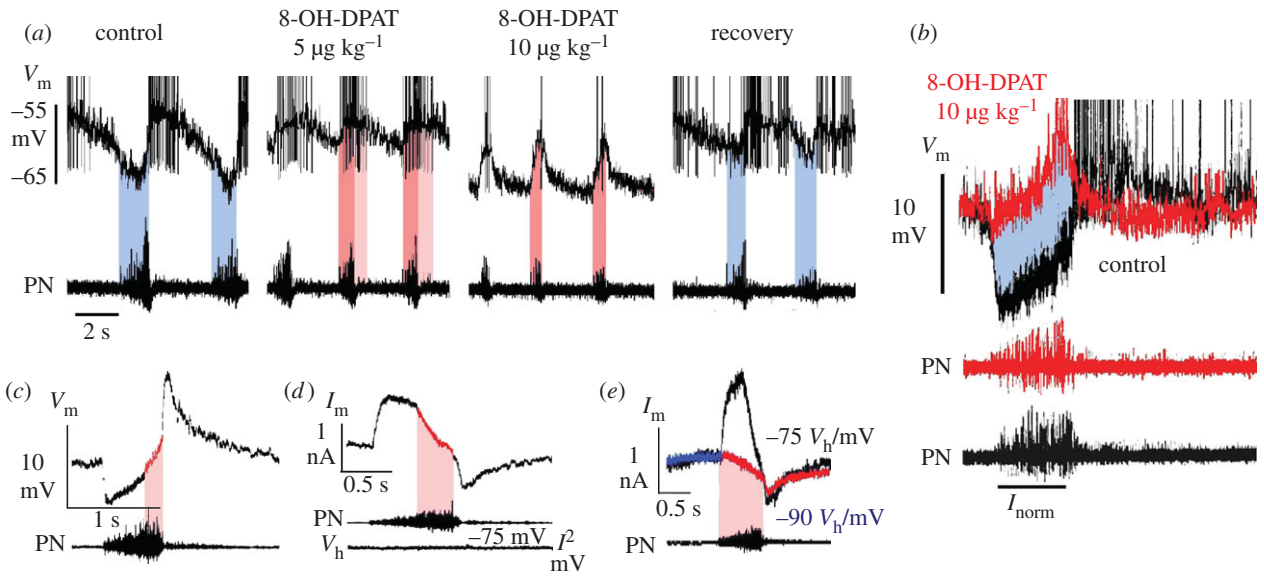

Figure 3. Modulation of inhibitory synaptic interactions within the respiratory network of anaesthetized *in vivo* cats. (*a* and *b*) Two examples for the response of post-inspiratory (post-I) neurons with a mean membrane potential of −65 and −70 mV recorded within the rostral portion (3.5–4.0 mm rostral to obex) of the ventral respiratory group to systemic application of the 5-HT_{1A}R agonist 8-OH-DPAT. Post-I neurons normally receive the most powerful synaptic inhibition during inspiration, when phrenic nerves (PN) reveal an augmenting burst discharge (blue time periods). Applying 8-OH-DPAT systemically at increasing concentrations (5 µg kg^{-1} amounts) induces the release of post-I neurons from inspiratory synaptic inhibition enabling them to discharge action potentials not only post-inspiration, but also during inspiration (pink time periods). At higher concentrations of 8-OH-DPAT (10–50 µg kg^{-1}), post-I neurons hyperpolarize and their action potential firing is limited to the inspiratory phase (pink time window). The release from inspiratory inhibition and activity shifting of post-I discharge into inspiration is illustrated by superposed traces at a time scale that is normalized to inspiratory duration in (*b*). (*c*) *In vivo* single-cell voltage-clamp analyses of post-I neurons show an inhibitory outward current during early inspiration that turns to a clear inward shift later in inspiration, which indicates the integration of inhibitory outward and excitatory inward currents. (*d*) The existence of an excitatory synaptic current during inspiration becomes apparent when the membrane potential is held close to the presumed chloride equilibrium potential, which exposes a clear inward current which begins at the start of inspiration (*e*).

fixed for 4 h and then cryoprotected with 30 per cent sucrose. Series of 20 and 40 µm thick transverse brainstem sections were cut using a cryostat (Frigocut, Reichert-Jung, Germany).

The following primary antibodies were diluted (1–5 µg ml^{-1}) in a solution containing 2 per cent (w/v) BSA in phosphate-buffered saline (PBS) and applied for 48–72 h at 4°C: affinity-purified hamster monoclonal antibody against 5-HT_7R (clone 5HTR7/220), guinea pig polyclonal antibody against 5-HT_{1A}R (AB5406; Millipore), rabbit polyclonal GlyT2 antibody (G8168-21; US Biologicals) and goat polyclonal antibody against µ-OR (sc-7488; Santa Cruz), goat polyclonal antibody against choline acetyltransferase (Millipore) and guinea pig polyclonal antibody against NK-1R (AB15810; Chemicon). After incubation, the sections were rinsed three times in PBS and subsequently incubated for 4 h in 2 per cent (w/v) BSA in PBS containing species-specific secondary antibodies conjugated with Cy2, Cy3, or Cy5 (Dianova) at a dilution of 1 : 500. The analysis of the neuronal immunofluorescence was performed with a confocal laser-scanning microscope LSM 510 Meta (Zeiss, Göttingen, Germany). For data acquisition and analysis of the confocal images, we used the LSM 510 META software (Zeiss, Germany). Subsequent imaging procedures (cell counting) were performed using IMAGEJ (http://rsb.info.nih.gov/ij/).

(h) *Real-time PCR*

For real-time RT–PCR analysis, we dissected the pre-BötC that was identified by the appearance of the principal nucleus of the inferior olive from corresponding cryostat sections cut in a rostro-caudal extension of 300 µm ($n = 3$, two patches from both sides of three juvenile Sprague-Dawley rats, P30). Total RNA was isolated using the Trizol method (Invitrogen) according to manufacturer's instructions and quantified using a nanodrop ND-1000 spectrophotometer. RNA quality and integrity was assessed by electrophoresis using an RNA 6000 LabChip kit and an Agilent 2100 Bioanalyzer. First-strand cDNA was synthesized using the iScript cDNA Synthesis Kit (BioRad). Primer pairs were designed using the Primer3 program (http://frodo.wi.mit.edu/cgi-bin/primer3/primer3_www.cgi): hypoxanthine guanine phosphoribosyl transferase (NM_012583, 135 bp; Hprt-F: 5′-gtcaagcagtacagccccaaaatg-3′, Hprt-R: 5′-gtcaagggcatatccaacaacaaac-3′), 5-HT_{1A}R (NM_012585, 161 bp, Htr1a-F: 5′-cacggctacaccatctactc-3′, Htr1a-R: 5′-gacgaagttcctaagctggt-3′), 5-HT_7R (NM_022938, 193 bp, Htr7-F: 5′-tgcaaactctctcattaatcct-3′, Htr7-R: 5′-ggtcagagttttgtcttacagc-3′), GlyT2 (NM_203334, 210 bp, Slc6a5-F: 5′-atgatgctggcactggctggctta-3′, Slc6a5-R: 5′-agacacaaaagaagcaaacaggt-3′) and µ-OR (NM_013071, 208 bp, Oprm1-F: 5′-gtggtcgtggctgtatttat-3′, Oprm1-R:

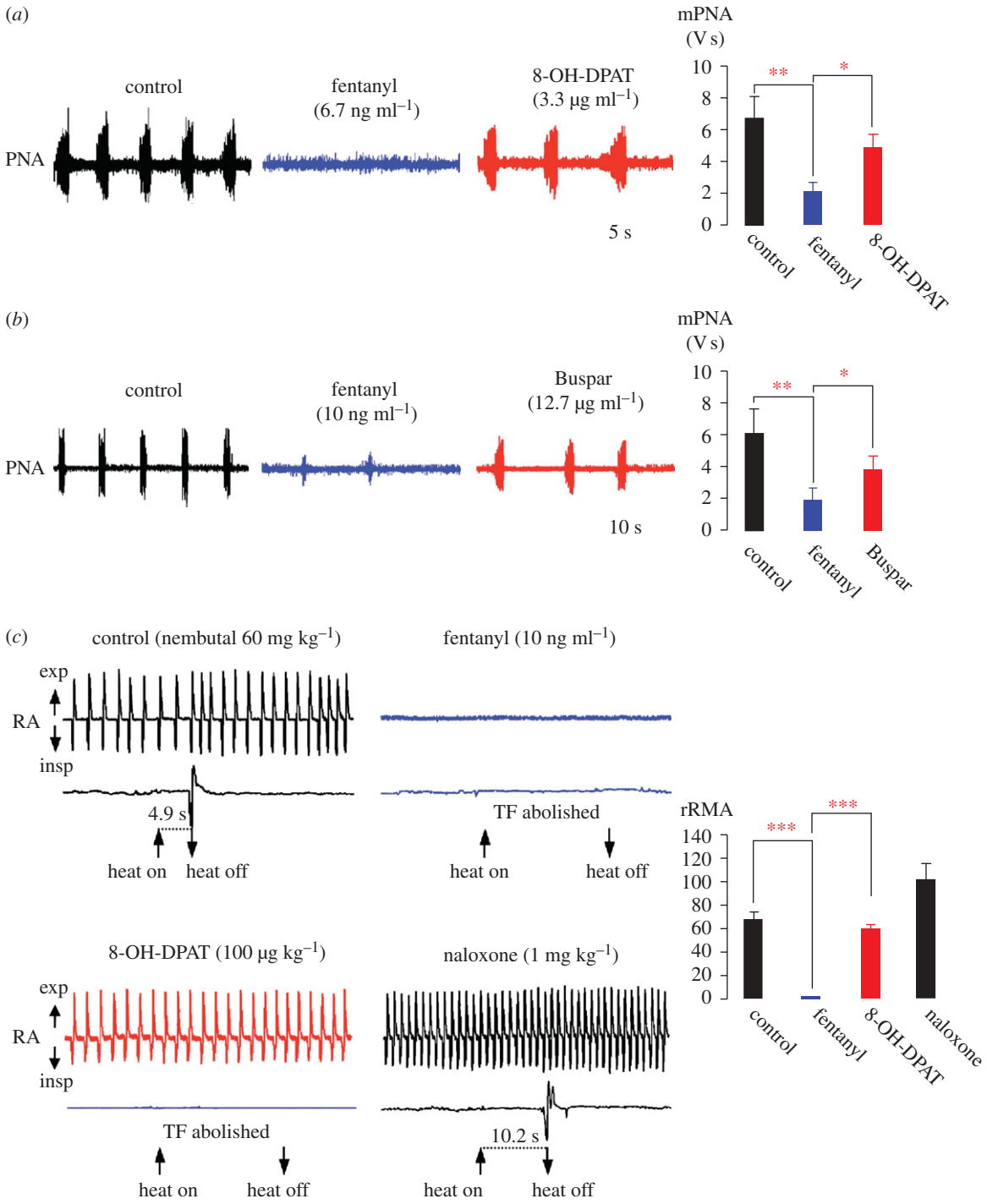

Figure 4. Treatment of opioid-induced depression of respiratory activity with 5-HT_{1A}R agonists in rats. Treatment of perfused brainstem–spinal cord preparation with 8-OH-DPAT (*a*) and the clinically approved 5-HT_{1A}R agonist buspirone (Buspar; *b*). Both drugs overcome fentanyl-provoked depression of rhythmic PNA. (*a*) Systemic administration of fentanyl (6.7 ng ml^{-1}) significantly reduced or blocked PNA (blue trace). Subsequent application of 8-OH-DPAT (3.3 µg ml^{-1}) recovered PNA to control levels (red trace). (*b*) A comparable action is shown for Buspar. (*c*) Systemic treatment with 5-HT_{1A}R agonist reverses opioid-provoked depression of breathing without affecting analgesia. Relative changes of rRMA were measured in anaesthetized, fully intact rats. Black trace shows spontaneous breathing and heat-provoked TFR under control conditions. Application of the μ-OR agonist fentanyl (10 µg kg^{-1}) induced apnoea and the TFR was completely blocked (blue trace). Application of 8-OH-DPAT (100 µg kg^{-1}) reinstated breathing, which increased steadily towards control levels (red trace). However, TFR remained abolished. The μ-OR antagonist naloxone (1 mg ml^{-1}) induced an increase in rRMA above control levels and restored the TFR after a short latency (black trace). Statistical analysis is denoted in the histograms in the panels on the right, with asterisks indicating significance (*$p < 0.05$; **$p < 0.01$; ***$p < 0.001$).

5′-ggatgcagaactctctgaag-3′). Gel electrophoresis revealed a single PCR product, and melting curve analysis showed a single peak for all amplification products. As an additional control, all PCR products were sequenced to confirm the identity of each amplicon. Ten-fold serial dilutions generated from pooled cDNA from all samples were used as a reference for the standard curve calculation to determine primer efficiency. Triplicates of all

real-time PCR reactions were performed in 25 µl reactions containing 1/20 dilution of the sample cDNA preparation from 250 ng total RNA, 400 nM of each primer, and 1 × iQ-SYBR Green Supermix (BioRad Laboratories, Ltd). The PCR reactions were cycled as follows: initial denaturation at 95°C for 10 min, 40 cycles of (denaturation 95°C/15 s, annealing 55°C/15 s, extension 72°C/30 s) and a final gradual increase of 0.5°C in temperature from 55°C to 95°C. All real-time quantifications were performed with the iCycler iQ system (BioRad) and were analysed by using a two-tailed paired *t*-test following normalization to the Hprt control.

(i) *Single-cell RT–PCR*

To harvest cytosol for RT–PCR analysis, cells were patched and identified as inspiratory neurons. Patch pipettes were filled with internal solution containing (in mM): 120 K^+-gluconate, 15 NaCl, 2 $MgCl_2$, 10 HEPES, 0.5 Na_2ATP, 1 $CaCl_2$, 3 1,2-bis-(2-aminophenoxy)ethane-*N*, *N*, *N*′,*N*′-tetraacetic acid, pH 7.4 adjusted with KOH; solution osmolarity ranged from 285 to 290 mOsm. To allow a diffusional exchange of cytosol and pipette solution, cells were held in the whole-cell configuration for at least 15 min. Subsequently, the cytoplasm was aspirated under visual control, while the access resistance was monitored to verify intact gigaseal formation. After breaking the gigaseal, the pipette was immediately withdrawn from the slice. Reverse transcription was carried out for 10 min at 25°C followed by incubation for 50 min at 42°C (SuperScript II reverse transcriptase; Invitrogen). The PCR amplification was performed with specific primers. All primers were tested on plasmid (5-HT_{1A} and 5-HT_7 receptors) as well as on total brain cDNA (5-HT_{1A}, 5-HT_7 and µ-ORs). The primer concentration for all amplification reactions was 0.2 µM. The cycling conditions for the amplification with AmpliTag Gold polymerase (Applied Biosystems) were a hot start at 95°C for 10 min, 40 cycles at 94°C for 30 s, 56°C for 30 s, 72°C for 1 min and an elongation step at 72°C for 10 min. In parallel, PCR was also performed with the AccuPrime Taq DNA polymerase system (Invitrogen), 94°C for 2 min followed by 39 cycles denaturation (94°C for 30 s), annealing (55°C for 30 s) and elongation (68°C for 1 min). The following primer pairs were used for the specific amplification of 5-HT_{1A}R (Htr1a-F: 5′-tctgcccagcgaggctggtc-3′ and Htr1a-R: 5′-gatcctgtagcctcgactg-3′), 5-HT_7R (Htr7-F: 5′-gagtcgagaaagttgtgatcggctcca-3′ and Htr7-R: 5′-aggtacctgtcaatgctgatcacgcac-3′), µ-OR (Oprm1-F: 5′-ttctgcattgctttgggttacacg-3′ and Oprm1-R: 5′-ctgacagcaacctgattccacgta-3′), and β-actin (Actb-F: 5′tggccttagggttgcaggggg-3′ and Actb-R: 5′-gtgggccgctctaggcacca-3′).

(j) *Statistics*

All statistical tests were performed with repeated ANOVA followed by a Fisher LSD *post hoc* test using SYSTAT 8 software (SPSS Inc., Chicago, IL, USA).

3. RESULTS

(a) *5-HTR expression on inhibitory interneurons*

Single-cell RT-PCR analysis of the cytosol harvested from identified inspiratory neurons (figure 1*a*) in the brainstem slice preparation of rat revealed the presence of µ-OR, 5-HT_{1A}R and 5-HT_7R transcripts (figure 1*b*). The expression levels related to the housekeeping gene *Hprt* of the two 5-HTR transcripts were similar (5-HT_{1A}R, 0.99 ± 0.22; 5-HT_7R, 1.14 ± 0.17), and significantly lower for the neuronal glycine transporter GlyT2 (0.43 ± 0.07).

At the protein level, we studied the cellular expression patterns of 5-HT_{1A}R and 5-HT_7R. A novel anti-peptide monoclonal antibody recognizing 5-HT_7R was developed using Phe^{281}–Gly^{294} (NH_2-FPRVQPESVISLNG-COOH) in the third intracellular loop of the rat 5-HT_7R as an antigen for immunization (figure 1*c*). This antibody was used in combination with commercially available antibodies recognizing 5-HT_{1A}R and GlyT2, the neuronal glycine transporter, for specific labelling of inhibitory glycinergic neurons (figure 1*e*,*f*). To obtain a complete overview of receptor expression profiles in excitatory and inhibitory neurons, immunohistochemistry was performed using sections encompassing the entire 200 µm extension of the pre-BötC (including five consecutive 40 µm thick transverse sections; $n = 5$ animals) counting in total 2438 neurons within the pre-BötC (figure 1*e*). The analysis revealed that a large percentage (62.4%) of pre-BötC neurons are glycinergic, as they show GlyT2 immunoreactivity. The majority of these glycinergic neurons also expressed 5-HT_{1A}R (79.9%), while 73.9 per cent of neurons expressed 5-HT_7R. Only 18.7 per cent of cells solely expressed 5-HT_{1A}R, and 12.7 per cent expressed only 5-HT_7R. A minority (7.4%) of cells lacked either 5-HT receptor. The remaining 37.6 per cent of pre-BötC cells may comprise glutamatergic or GABAergic neurons. The expression of 5-HT_{1A}R and 5-HT_7R was also high in the GlyT2-negative group of cells, 84.6 per cent of cells expressing 5-HT_{1A}Rs and 74.8 per cent of cells expressing 5-HT_7Rs. A large portion of GlyT2-positive neurons also co-expressed µ-OR (figure 1*f*). The inference is that glycinergic neurons in the pre-BötC network do not only transmit, but evidently also receive signals via glycine receptors.

(b) *Network responses to 5-HTR-specific signalling*

Following the observation that breathing is highly sensitive to opioids as well as a variety of 5-HTR signalling pathways, we tested for pharmacological effects of selective 5-HT_{1A}R and 5-HT_7R activation. The rationale was that agonists such as 8-OH-DPAT might also activate G_s-coupled 5-HT_7Rs (Hedlund *et al.* 2004) and coactivation of these 5-HT_7Rs might prevail over the inhibitory $G_{i/o}$–AC pathway to neutralize the 5-HT_{1A}R-induced decline of intracellular cAMP levels (Hoyer *et al.* 2002).

We tested for 5-HT_7R- and 5-HT_{1A}R-specific effects in the perfused rat brainstem–spinal cord

preparation, in which the respiratory network remains fully intact (Paton 1996). The network response was measured by recording phrenic nerve activity (PNA) and deriving minute respiratory activity (mPNA) online, before and after administering 5-HT_{1A}R or 5-HT_7R agonists or antagonists. Surprisingly, application of the 5-HT_7R agonist 5-CT (0.3 $\mu g\,ml^{-1}$) did not activate, rather it significantly reduced, mPNA (from 10.42 ± 3.98 to 4.47 ± 1.77; $n = 5$). mPNA activity was suppressed further (to 0.96 ± 0.41) when 5-HT_{1A}R were additionally blocked with the selective antagonist WAY 100635 (figure 2*a*). Conversely, mPNA was augmented when the agonist 8-OH-DPAT was administered after 5-HT_7Rs had been blocked with SB 269970 (figure 2*b*). Augmentation of mPNA activity occurred by enhanced burst frequency (9.54 ± 0.20 V s; $p < 0.05$) rather than an increase in PNA burst amplitude. Notably, the 5-HT_{1A}R-dependent enhancement of PNA frequency by 8-OH-DPAT was abolished when glycine receptors were blocked by systemic application of strychnine. Strychnine application itself provoked a significant increase of mPNA (from 13.33 ± 1.03 to 22.73 ± 4.44; $p < 0.05$; $n = 5$), which did not change further (21.40 ± 4.64) when 5-HT_{1A}Rs were additionally activated by 8-OH-DPAT (figure 2*c*).

Results were quite similar when relative changes of respiratory minute airflow (rRMA) were measured *in vivo* in anaesthetized rats. Administration of 8-OH-DPAT ($n = 5$) enhanced rRMA to 187 per cent (from 58.2 ± 8.4 to 109.3 ± 9.2; $p < 0.01$), an effect that was blocked by the 5-HT_{1A}R-antagonist WAY 100635 ($n = 3$; figure 2*d*).

Taken together, these data demonstrate that the 8-OH-DPAT-induced increase of mPNA originates from a 5-HT_{1A}R-specific modulation and is not simply explained by a 5-HT_7R antagonism. The surprising network responses to 5-HT_{1A}R and 5-HT_7R stimulation, together with their disappearance after strychnine application, suggests that there is a signal-reversing process mediated through modulation of glycinergic inhibition.

(c) *Modulation of inhibitory synaptic processes during global 5-HT_{1A}R modulation*

To test for 5-HT_{1A}R-specific modulation of inhibitory synaptic processes, single-electrode current- and voltage-clamp measurements of identified respiratory brainstem neurons were performed in pentobarbital-anaesthetized cats. In contrast to augmentation of synaptic inhibition by single-cell electrophoresis of 5-HT_{1A}R agonists (Lalley *et al.* 1994; Richter *et al.* 1997), global activation of 5-HT_{1A}Rs by intravenous injection of 8-OH-DPAT provoked an increase in neuronal excitability owing to a diminution of synaptic inhibition as tested in expiratory ($n = 12$) and post-inspiratory (post-I; $n = 4$) neurons within brainstem coordinates that outline the localization of the preBötC in cat (Schwarzacher *et al.* 1995). The reduction in synaptic inhibition was most obvious in post-I neurons (figure 3), which are known to be glycinergic (Schmid *et al.* 1991; Ezure *et al.* 2003). These post-I neurons exhibited a release from early-inspiratory synaptic inhibition, causing them to advance their action potential firing far into the preceding inspiratory phase of the oscillatory cycle (figure 3*a*,*c*). At higher concentrations of 8-OH-DPAT, this release from early-inspiratory inhibition was combined with a membrane hyperpolarization, which limited action potential discharge to the late-inspiratory period, when post-I neurons are normally effectively silenced (figure 3*a*,*b*). *In vivo* voltage-clamp measurements performed at holding voltages of -75 to -90 mV, which is close to the chloride (inhibitory post-synaptic current) equilibrium potential (Haji *et al.* 2000), uncovered a clear inward current component, revealing that the process enabling the 8-OH-DPAT-provoked activity shift is linked to an excitatory synaptic input during inspiration. Under control conditions such an excitatory drive seemed to be shunted by synchronous synaptic inhibition (figure 3*c*–*e*).

The 5-HT_{1A}R-induced change in the inspiratory phase-terminating discharge of inhibitory post-I neurons (Richter *et al.* 1987) is consistent with the corresponding network response to 8-OH-DPAT recorded from the phrenic nerve, consisting of shortened inspiratory burst duration and increased burst frequency (figure 3*a*). It is noteworthy that a similar effect has been described after strychnine blockade of glycinergic synaptic transmission (Busselberg *et al.* 2003).

(d) *Network responses to parallel 5-HT_{1A}R and opiate receptor signalling*

The perception that the activation of rhythmic network output is accomplished by disinhibition of glycinergic neurons that could counteract opioid-induced depression of respiratory activity was confirmed with a sequential strategy of pharmacological treatment in the *in situ* perfused rat brainstem preparation. Opiate treatment was used to depress respiratory PNA, followed by the systemic administration of 8-OH-DPAT or buspirone, which is a clinically approved partial 5-HT_{1A}R agonist (figure 4). After fentanyl had significantly reduced or arrested mPNA (from 6.76 ± 1.41 to 2.11 ± 0.58; $p < 0.01$), systemic administration of 8-OH-DPAT recovered mPNA to approximately 70 per cent of normal activity levels (4.95 ± 0.87 compared with 6.76 ± 1.41; $p < 0.05$; $n = 6$; figure 4*a*). The fentanyl-induced depression of mPNA (1.93 ± 0.73 versus 6.17 ± 1.55 V s; $p < 0.01$) was effectively re-activated with successive administration of buspirone (3.88 ± 0.88; $p < 0.05$; $n = 4$; figure 4*b*).

The recovery from opioid-depressed respiratory activity as seen in wild-type rodents was also verified *in vivo*. The μ-OR-agonist fentanyl, which is sufficient to completely block the nociceptive TF reflex (TFR; defined as a threefold prolongation of the 7.35 ± 1.11 s TFR at control), induced apnoea in rats (figure 4*c*). Subsequent administration of 8-OH-DPAT restored breathing within 2–3 min (figure 4*c*). The relative rRMA reappeared with 0.21 ± 0.4 ($p < 0.001$) and increased steadily within the following 3 min (0.60 ± 0.03 compared with control values of 0.68 ± 0.06; $p < 0.001$), while the TFR was not restored. This effect was μ-OR specific, because the

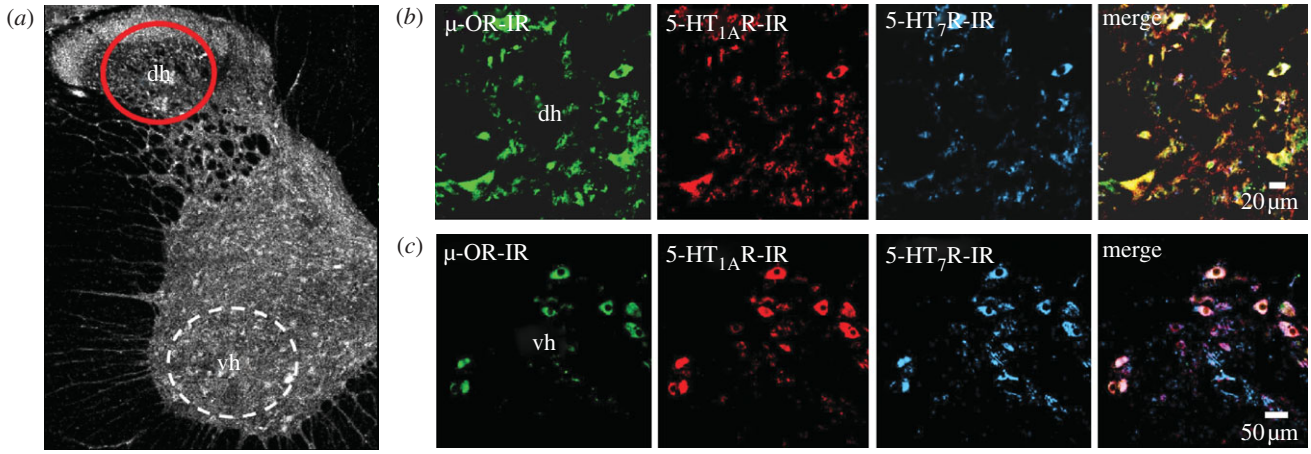

Figure 5. 5-HT_{1A}, 5-HT_7, and μ-OR expression in dorsal horn neurons of the rat spinal cord. Triple-labelling of 5-HT_{1A}, 5-HT_7 and μ-ORs in 40 μm thick sections from the cervical spinal cord (spinal segment C3/C4; overview in *a*) revealed with a goat anti-μ-OR antibody, a guinea pig anti-5-HT_{1A}R antibody and a hamster anti-5-HT_7R antibody (clone 5HTR7/220) and appropriate fluorochrome-conjugated secondary antibodies: μ-OR (Cy2, green), 5-HT_{1A}R (Cy3, red) and 5-HT_7R (Cy5, blue). Within the dorsal horn (dh, *b*) the majority (95.1%) of μ-OR-immunoreactive neurons expressed 5-HT_{1A}R, while only 53.4 per cent coexpressed 5-HT_7R. The 5-HT_{1A}, 5-HT_7 and μ-ORs were strongly coexpressed in neurons of the ventral horn (vh, *c*).

antagonist naloxone induced an increase in rRMA above control levels (1.03 ± 0.12 versus 0.68 ± 0.06) and also fully restored the TFR (figure 4*c*).

(e) *Receptor expression in the nociceptive dorsal horn network*

Real-time PCR analysis from total cervical spinal cord tissue of the segments C2–C4 revealed relative transcript levels of 1.09 ± 0.16 for 5-HT_{1A}R, 1.04 ± 0.29 for 5-HT_7R and 0.88 ± 0.12 for μ-OR. Immunohistochemical analysis of protein expression (five sections from five animals each) showed that 95.1 per cent of the μ-OR-immunoreactive dorsal horn neurons are also positive for the 5-HT_{1A}R, whilst 5-HT_7R was detected only in 53.4 per cent of cells (figure 5). Such strong colocalization of μ-ORs and 5-HT_{1A}Rs implies that synergistic signalling effectively reduces cellular cAMP that may account for a failure of nociceptive signalling in dorsal horn neurons.

4. DISCUSSION

Global administration of cAMP-depressing modulators into a neuronal network that operates by synaptic interactions between excitatory and inhibitory neurons can be expected to induce depression of neuronal excitability that also provokes particular forms of disinhibition. These synaptic interaction-dependent effects are evident in the respiratory network, which operates with a reciprocal organization of antagonistic groups of glutamatergic, GABAergic and glycinergic interneurons (Richter 1996). The outcome of synaptic disinhibition depends on the specific action of these inhibitory interneurons (figure 6) whose contribution is revealed by the glycine and $GABA_A$ receptor antagonists—strychnine and bicuculline (Schmid *et al.* 1996; Busselberg *et al.* 2001). Modulation of glycinergic inhibition seems particularly effective, because it not only controls patterning of the steadily augmenting inspiratory (aug-I) and expiratory (aug-E) burst discharges, but also regulates the efficiency of respiratory phase control by early-inspiratory (early-I) and post-inspiratory (post-I) neurons (Richter 1982; Busselberg *et al.* 2001; Ezure *et al.* 2003; figure 6*a*). Glycinergic control of respiratory phase termination is vital (Pierrefiche *et al.* 1998) and, therefore, it is not surprising that more than 60 per cent of neurons within the pre-BötC are glycinergic, as identified by the neuronal glycine transporter GlyT2 (Gomeza *et al.* 2003; Tanaka *et al.* 2003). Some of these GlyT2-labelled inhibitory neurons were identified as respiratory in whole cell recordings (Winter *et al.* 2009). The GlyT2-positive inhibitory neurons also express 5-HT_{1A}R and 5-HT_7R (figure 1) and, therefore, are subjected to ongoing modulatory control by serotonin that is continuously released from raphé neurons (Connelly *et al.* 1989; Mason *et al.* 2007). Another important finding is that inhibitory glycinergic neurons themselves receive glycinergic inhibitory inputs (figure 1). This makes disinhibition a critical process in network adjustment.

A predominant modulatory effect of 5-HT is exerted through 5-HT_{1A}R that is expressed in 80 per cent of all pre-BötC cells. A commonly used drug to test for the functional consequences of 5-HT_{1A}R modulation is the agonist 8-OH-DPAT. When respiratory neurons are tested individually with locally restricted ionophoretic application of 8-OH-DPAT or with drugs that inhibit cAMP-dependent protein kinase A (PKA), individual neurons respond equally well with a significant enhancement of inhibitory synaptic currents (Lalley *et al.* 1997). This is particularly clear for the glycinergic processes mediated by post-I neurons (Richter *et al.* 1987, 1992) and such pronounced enhancement of glycinergic synaptic currents (Lalley *et al.* 1997; Richter *et al.* 1997) must be expected to alter the operation of the whole respiratory network. We propose a reorganization of network operation as is schematically shown in figure 6*b*. Discharge of early-I neurons is evidently abolished,

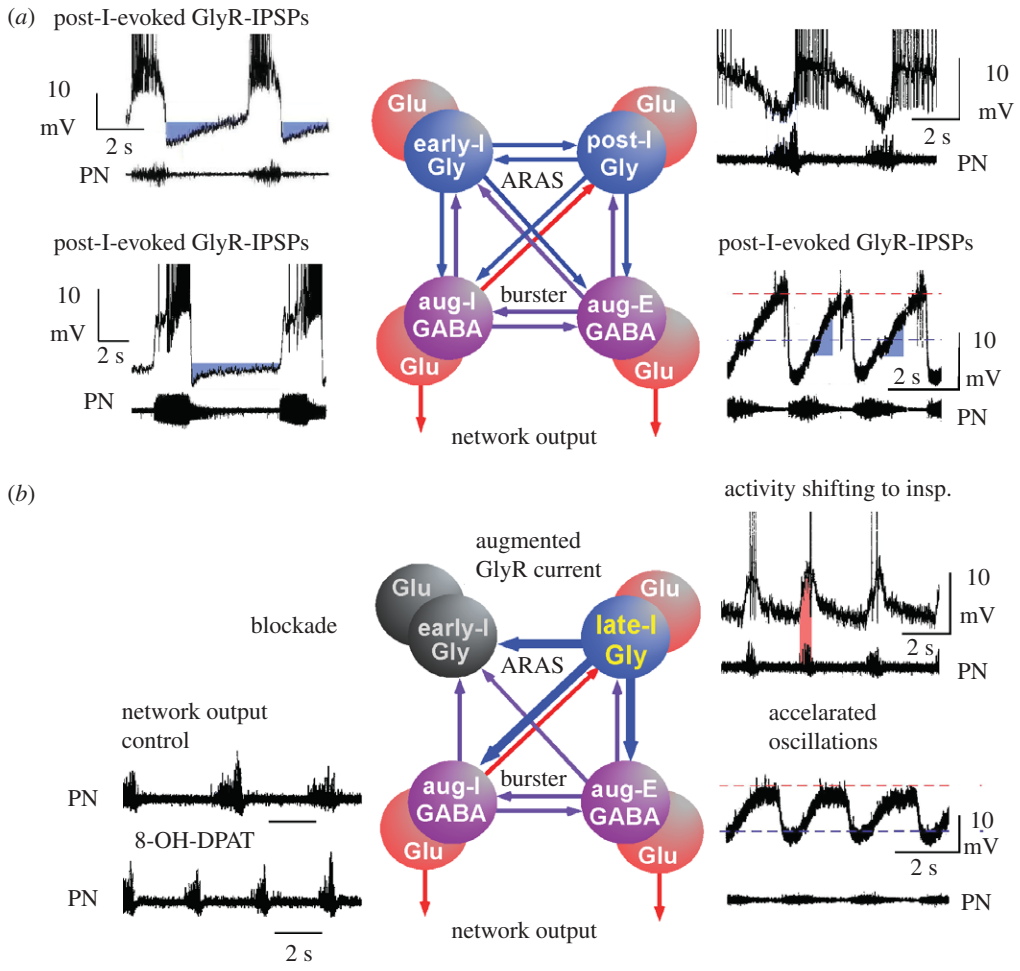

Figure 6. Proposal of the network reorganization following global stimulation of 5-HT_{1A}R. Based on the experimental data obtained in mouse, rat and cat, we propose a functional reorganization of network operation. (*a*) Starting from control, we conclude that the respiratory network reveals a mutual inhibitory organization between antagonistic groups of neurons operating either via GABAergic synaptic interaction (violet cells and arrows) or through glycinergic interactions (blue cells and arrows (ARAS, ascending reticular activating system; IPSPs, inhibitory postsynaptic potentials)). Activation of both inhibitory processes is fully controlled by excitatory glutamatergic neurons (red cells) that determine the neural output to respiratory and laryngeal muscles through polysynaptic bulbar and bulbo-spinal connections. GABAergic and glycinergic neurons form the indispensable structure for mutual inhibition. There is a reciprocal GABAergic synaptic interaction between inspiratory (aug-I) and expiratory (aug-E) neurons generating an alternating pattern of augmenting activity that is necessary for breathing movements. Equally important seem to be the inhibitory interactions between early-inspiratory (early-I) and post-inspiratory (post-I) neurons that control phase transitions between respiratory cycles. In the original recordings (from cat) depicted beside each neuron population, hyperpolarizing voltage trajectories generated by glycinergic inhibition of the different types of neurons are labelled in blue. (*b*) 5-HT_{1A}R-mediated signalling induces a functional reorganization of network operation that originates from a potentiation of glycine receptors (GlyR) as illustrated by thick arrows indicating synaptic interconnections. The firing of post-I neurons shifts into the inspiratory phase (inset of original recording, pink area), which seems to powerfully suppress early-I neuronal discharges by enhanced GlyR currents. Suppression of early-I neurons is evidenced by the disappearance of inspiratory inhibition of post-I neurons. As post-I neurons fire prematurely during inspiration, enhanced glycinergic inhibition of aug-I neurons effectively shortens inspiratory burst duration, but increases burst frequency of inspiratory neurons as seen in the inspiratory output in the phrenic nerves (PN).

because their inhibitory feedback to post-I neurons disappears (figure 3*a*). Disinhibition of post-I neurons causes a fundamental change in network operation, because it induces a notable shift of post-I neuronal firing into the preceding inspiratory phase (figure 6*b*, see also figure 3). Their time-shifted and prolonged discharge is supposed to be very efficient, because 5-HT_{1A}R-induced modulation potentiates inhibitory synaptic currents in the innervated neurons (Lalley *et al.* 1997). These effects are only partially reduced but not abolished at higher 8-OH-DPAT concentrations when post-I neurons undergo a gK^+-controlled membrane hyperpolarization (Lalley *et al.* 1994; Ballanyi *et al.* 1997) limiting their discharge to late-inspiratory periods.

The functional uncoupling of early-I neurons from the network, combined with phase-shifting of post-I firing into the inspiratory phase, leads to the disappearance of normal post-inspiratory activity and provokes a two-phased oscillation between inspiration and expiration. This is consistent with the observation that 5-HT_{1A}R-evoked modulation is greatly

reduced when glycine receptors were blocked by strychnine (figure 1*d*), while an identical 'phase-shifting' occurs in the discharge of post-I neurons (Busselberg *et al.* 2001; Dutschmann & Paton 2002). Post-I neurons originating from the pons (Dick *et al.* 1994; Dutschmann & Herbert 2006) should be modulated synergistically. A minor change in network excitability might occur by modulation of tonically active glycinergic inputs (Haji *et al.* 1992). In conclusion, the data suggest that glycinergic synapses are the critical target of 5-HT_{1A}R-regulated modulation of network functions and that reinforcement of inhibitory glycinergic processes (Lalley *et al.* 1997) might protect against arrhythmic breathing disturbances.

μ-ORs are abundantly expressed in pre-BötC neurons (Manzke *et al.* 2003) including NK-1R-positive excitatory neurons (Gray *et al.* 1999) and GlyT2-positive inhibitory respiratory neurons (figure 1). When activated, μ-ORs depress neuronal excitability of all these cell types (Ballanyi *et al.* 1997; Mellen *et al.* 2003). At opioid concentrations sufficient to slow respiration, respiratory periods are prolonged, indicating that the onset of post-I neuronal discharge is delayed and burst duration is lengthened (Lalley 2006). Such suppressed post-I neuronal discharge seems to be insufficient for adequate termination of the inspiratory phase. Our finding of a 5-HT_{1A}R-induced disinhibition of post-I neurons (figure 3), enabling them to shift their discharge into the preceding inspiratory phase and potentiation of their inhibitory postsynaptic currents, appears to significantly shorten the latency of inspiratory phase termination and thus the rescue of respiratory rhythmicity. The present experiments demonstrate that this effect is fairly robust and compensates for μ-OR-induced depression of neuronal bursting (Brunton & Charpak 1997; Wagner *et al.* 2000; Chieng *et al.* 2006). Further analyses are necessary to understand how the accompanying membrane hyperpolarization affects membrane properties necessary for endogenous and/or rebound bursting (Ramirez & Richter 1996; Ramirez *et al.* 1997; Butera *et al.* 1999; Del Negro *et al.* 2002).

(a) *Anti-nociceptive effect of 5-HT_{1A}R agonists*

In the sensory network of spinal nociceptive dorsal horn neurons, our immunohistochemical analysis showed that 95.1 per cent of the μ-OR-immunoreactive neurons coexpress 5-HT_{1A}Rs, while only 53.4 per cent of neurons express 5-HT_7Rs (see figure 5). Therefore, the effects of 5-HT_7Rs must be weaker, because the synergistic actions of μ-ORs and 5-HT_{1A}Rs should effectively depress cellular cAMP levels in this population of neurons. This should diminish PKA-dependent phosphorylation of the glycine receptors (Harvey *et al.* 2004) and potentiate synaptic inhibition to further enhance anti-nociception (Sandkuhler *et al.* 1987; Helmchen *et al.* 1995).

(b) *Significance for translational medicine*

The present analyses of molecular, cellular and systemic processes reveal that in the case of reciprocally wired networks, predominant modulation of inhibitory neurons can prevail over depression of excitatory neurons to initiate a functional reorganization of the operational network machinery (figure 6*c*). The significance of such self-reorganization is evident in the respiratory network and explains how fentanyl depression of respiratory rhythmicity can be overcome with 5-HT_{1A}R agonists (Sahibzada *et al.* 2000; Meyer *et al.* 2006). An important inference can be drawn: 5-HT_{1A}R agonists may effectively protect against opiate-induced apnoea or severe slowing of breathing, but the underlying processes also induce a depression of inspiratory peak activity that affects tidal volume. Therefore, there is the possibility that the treatment could result in shallow breathing, which would require additional medical treatment.

The animal experiments were performed in accordance with the European Community and National Institutes of Health guidelines for the care and use of laboratory animals and were approved by the Ethics Committee of the Georg-August-University, Göttingen, Germany.

This work was supported by the DFG Research Center Molecular Physiology of the Brain (CMPB; FZT 103) and by the German Ministry for Education and Science (BMBF) via the Bernstein Center for Computational Neuroscience (BCCN) Göttingen under grant no. 01GQ0432. We are grateful to Anna-Maria Bischoff for excellent technical support during the course of the experiments.

REFERENCES

Ballantyne, D., Andrzejewski, M., Muckenhoff, K. & Scheid, P. 2004 Rhythms, synchrony and electrical coupling in the locus coeruleus. *Respir. Physiol. Neurobiol.* **143**, 199–214. (doi:10.1016/j.resp.2004.07.018)

Ballanyi, K., Lalley, P. M., Hoch, B. & Richter, D. W. 1997 cAMP-dependent reversal of opioid- and prostaglandin-mediated depression of the isolated respiratory network in newborn rats. *J. Physiol.* **504**, 127–134. (doi:10.1111/j.1469-7793.1997.127bf.x)

Bocchiaro, C. M. & Feldman, J. L. 2004 Synaptic activity-independent persistent plasticity in endogenously active mammalian motoneurons. *Proc. Natl Acad. Sci. USA* **101**, 4292–4295. (doi:10.1073/pnas.0305712101)

Brunton, J. & Charpak, S. 1997 Heterogeneity of cell firing properties and opioid sensitivity in the thalamic reticular nucleus. *Neuroscience* **78**, 303–307.

Busselberg, D., Bischoff, A. M., Paton, J. F. & Richter, D. W. 2001 Reorganisation of respiratory network activity after loss of glycinergic inhibition. *Pflugers Arch.* **441**, 444–449. (doi:10.1007/s004240000453)

Busselberg, D., Bischoff, A. M. & Richter, D. W. 2003 A combined blockade of glycine and calcium-dependent potassium channels abolishes the respiratory rhythm. *Neuroscience* **122**, 831–841. (doi:10.1016/j.neuroscience.2003.07.014)

Butera Jr, R. J., Rinzel, J. & Smith, J. C. 1999 Models of respiratory rhythm generation in the pre-Botzinger complex. I. Bursting pacemaker neurons. *J. Neurophysiol.* **82**, 382–397.

Chieng, B. C., Christie, M. J. & Osborne, P. B. 2006 Characterization of neurons in the rat central nucleus of the amygdala: cellular physiology, morphology, and opioid sensitivity. *J. Comp. Neurol.* **497**, 910–927. (doi:10.1002/cne.21025)

Connelly, C. A., Ellenberger, H. H. & Feldman, J. L. 1989 Are there serotonergic projections from raphe and retrotrapezoid nuclei to the ventral respiratory group in the

rat? *Neurosci. Lett.* **105**, 34–40. (doi:10.1016/0304-3940(89)90007-4)

Del Negro, C. A., Morgado-Valle, C. & Feldman, J. L. 2002 Respiratory rhythm: an emergent network property? *Neuron* **34**, 821–830. (doi:10.1016/S0896-6273(02)00712-2)

Dick, T. E., Bellingham, M. C. & Richter, D. W. 1994 Pontine respiratory neurons in anesthetized cats. *Brain Res.* **636**, 259–269. (doi:10.1016/0006-8993(94)91025-1)

Dutschmann, M. & Herbert, H. 2006 The Kolliker-Fuse nucleus gates the postinspiratory phase of the respiratory cycle to control inspiratory off-switch and upper airway resistance in rat. *Eur. J. Neurosci.* **24**, 1071–1084. (doi:10.1111/j.1460-9568.2006.04981.x)

Dutschmann, M. & Paton, J. F. 2002 Glycinergic inhibition is essential for co-ordinating cranial and spinal respiratory motor outputs in the neonatal rat. *J. Physiol.* **543**, 643–653. (doi:10.1113/jphysiol.2001.013466)

Ezure, K., Tanaka, I. & Kondo, M. 2003 Glycine is used as a transmitter by decrementing expiratory neurons of the ventrolateral medulla in the rat. *J. Neurosci.* **23**, 8941–8948.

Gomeza, J., Ohno, K., Hulsmann, S., Armsen, W., Eulenburg, V., Richter, D. W., Laube, B. & Betz, H. 2003 Deletion of the mouse glycine transporter 2 results in a hyperekplexia phenotype and postnatal lethality. *Neuron* **40**, 797–806. (doi:10.1016/S0896-6273(03)00673-1)

Gray, P. A., Rekling, J. C., Bocchiaro, C. M. & Feldman, J. L. 1999 Modulation of respiratory frequency by peptidergic input to rhythmogenic neurons in the preBotzinger complex. *Science* **286**, 1566–1568. (doi:10.1126/science.286.5444.1566)

Haji, A., Takeda, R. & Remmers, J. E. 1992 Evidence that glycine and GABA mediate postsynaptic inhibition of bulbar respiratory neurons in the cat. *J. Appl. Physiol.* **73**, 2333–2342.

Haji, A., Takeda, R. & Okazaki, M. 2000 Neuropharmacology of control of respiratory rhythm and pattern in mature mammals. *Pharmacol. Ther.* **86**, 277–304. (doi:10.1016/S0163-7258(00)00059-0)

Harvey, R. J. *et al.* 2004 GlyR alpha3: an essential target for spinal PGE2-mediated inflammatory pain sensitization. *Science* **304**, 884–887. (doi:10.1126/science.1094925)

Hedlund, P. B., Kelly, L., Mazur, C., Lovenberg, T., Sutcliffe, J. G. & Bonaventure, P. 2004 8-OH-DPAT acts on both 5-HT1A and 5-HT7 receptors to induce hypothermia in rodents. *Eur. J. Pharmacol.* **487**, 125–132. (doi:10.1016/j.ejphar.2004.01.031)

Helmchen, C., Fu, Q. G. & Sandkuhler, J. 1995 Inhibition of spinal nociceptive neurons by microinjections of somatostatin into the nucleus raphe magnus and the midbrain periaqueductal gray of the anesthetized cat. *Neurosci. Lett.* **187**, 137–141. (doi:10.1016/0304-3940(95)11345-2)

Hoyer, D., Hannon, J. P. & Martin, G. R. 2002 Molecular, pharmacological and functional diversity of 5-HT receptors. *Pharmacol. Biochem. Behav.* **71**, 533–554. (doi:10.1016/S0091-3057(01)00746-8)

Lalley, P. M. 2006 Opiate slowing of feline respiratory rhythm and effects on putative medullary phase-regulating neurons. *Am. J. Physiol. Regul. Integr. Comp. Physiol.* **290**, R1387–R1396. (doi:10.1152/ajpregu.00530.2005)

Lalley, P. M., Bischoff, A. M. & Richter, D. W. 1994 5-HT-1A receptor-mediated modulation of medullary expiratory neurones in the cat. *J. Physiol.* **476**, 117–130.

Lalley, P. M., Pierrefiche, O., Bischoff, A. M. & Richter, D. W. 1997 cAMP-dependent protein kinase modulates expiratory neurons *in vivo*. *J. Neurophysiol.* 77, 1119–1131.

Lotsch, J., Skarke, C., Schneider, A., Hummel, T. & Geisslinger, G. 2005 The 5-hydroxytryptamine 4 receptor agonist mosapride does not antagonize morphine-induced respiratory depression. *Clin. Pharmacol. Ther.* **78**, 278–287. (doi:10.1016/j.clpt.2005.05.010)

Manzke, T., Guenther, U., Ponimaskin, E. G., Haller, M., Dutschmann, M., Schwarzacher, S. & Richter, D. W. 2003 5-HT4(a) receptors avert opioid-induced breathing depression without loss of analgesia. *Science* **301**, 226–229. (doi:10.1126/science.1084674)

Mason, P., Gao, K. & Genzen, J. R. 2007 Serotonergic raphe magnus cell discharge reflects ongoing autonomic and respiratory activities. *J. Neurophysiol.* **98**, 1919–1927. (doi:10.1152/jn.00813.2007)

Mellen, N. M., Janczewski, W. A., Bocchiaro, C. M. & Feldman, J. L. 2003 Opioid-induced quantal slowing reveals dual networks for respiratory rhythm generation. *Neuron* **37**, 821–826. (doi:10.1016/S0896-6273(03)00092-8)

Meyer, L. C., Fuller, A. & Mitchell, D. 2006 Zacopride and 8-OH-DPAT reverse opioid-induced respiratory depression and hypoxia but not catatonic immobilization in goats. *Am. J. Physiol. Regul. Integr. Comp. Physiol.* **290**, R405–R413. (doi:10.1152/ajpregu.00440.2005)

Paton, J. F. 1996 A working heart-brainstem preparation of the mouse. *J. Neurosci. Methods* **65**, 63–68. (doi:10.1016/0165-0270(95)00147-6)

Pierrefiche, O., Schwarzacher, S. W., Bischoff, A. M. & Richter, D. W. 1998 Blockade of synaptic inhibition within the pre-Botzinger complex in the cat suppresses respiratory rhythm generation *in vivo*. *J. Physiol.* **509**, 245–254. (doi:10.1111/j.1469-7793.1998.245bo.x)

Ramirez, J. M. & Richter, D. W. 1996 The neuronal mechanisms of respiratory rhythm generation. *Curr. Opin. Neurobiol.* **6**, 817–825. (doi:10.1016/S0959-4388(96)80033-X)

Ramirez, J. M., Telgkamp, P., Elsen, F. P., Quellmalz, U. J. & Richter, D. W. 1997 Respiratory rhythm generation in mammals: synaptic and membrane properties. *Respir. Physiol.* **110**, 71–85. (doi:10.1016/S0034-5687(97)00074-1)

Richter, D. W. 1982 Generation and maintenance of the respiratory rhythm. *J. Exp. Biol.* **100**, 93–107.

Richter, D. W. 1996 Neural regulation of respiration: rhythmogenesis and afferent control. In *Comprehensive human physiology* (eds R. Greger & U. Windhorst), pp. 2979–2095. Berlin, Germany: Springer Verlag.

Richter, D. W. & Spyer, K. M. 2001 Studying rhythmogenesis of breathing: comparison of *in vivo* and *in vitro* models. *Trends Neurosci.* **24**, 464–472. (doi:10.1016/S0166-2236(00)01867-1)

Richter, D. W., Ballantyne, D. & Remmers, J. E. 1987 The differential organization of medullary post-inspiratory activities. *Pflugers Arch.* **410**, 420–427. (doi:10.1007/BF00586520)

Richter, D. W., Ballanyi, K. & Schwarzacher, S. 1992 Mechanisms of respiratory rhythm generation. *Curr. Opin. Neurobiol.* **2**, 788–793. (doi:10.1016/0959-4388(92)90135-8)

Richter, D. W., Pierrefiche, O., Lalley, P. M. & Polder, H. R. 1996 Voltage-clamp analysis of neurons within deep layers of the brain. *J. Neurosci. Methods* **67**, 121–123. (doi:10.1016/0165-0270(96)00042-8)

Richter, D. W., Lalley, P. M., Pierrefiche, O., Haji, A., Bischoff, A. M., Wilken, B. & Hanefeld, F. 1997 Intracellular signal pathways controlling respiratory neurons. *Respir. Physiol.* **110**, 113–123. (doi:10.1016/S0034-5687(97)00077-7)

Richter, D. W., Schmidt-Garcon, P., Pierrefiche, O., Bischoff, A. M. & Lalley, P. M. 1999 Neurotransmitters and neuromodulators controlling the hypoxic respiratory

response in anaesthetized cats. *J. Physiol.* **514**, 567–578. (doi:10.1111/j.1469-7793.1999.567ae.x)

Sahibzada, N., Ferreira, M., Wasserman, A. M., Taveira-DaSilva, A. M. & Gillis, R. A. 2000 Reversal of morphine-induced apnea in the anesthetized rat by drugs that activate 5-hydroxytryptamine(1A) receptors. *J. Pharmacol. Exp. Ther.* **292**, 704–713.

Sandkuhler, J., Maisch, B. & Zimmermann, M. 1987 Raphe magnus-induced descending inhibition of spinal nociceptive neurons is mediated through contralateral spinal pathways in the cat. *Neurosci. Lett.* **76**, 168–172. (doi:10.1016/0304-3940(87)90710-5)

Schmid, K., Bohmer, G. & Gebauer, K. 1991 Glycine receptor-mediated fast synaptic inhibition in the brainstem respiratory system. *Respir. Physiol.* **84**, 351–361. (doi:10.1016/0034-5687(91)90129-7)

Schmid, K., Foutz, A. S. & Denavit-Saubie, M. 1996 Inhibitions mediated by glycine and GABAA receptors shape the discharge pattern of bulbar respiratory neurons. *Brain Res.* **710**, 150–160. (doi:10.1016/0006-8993(95)01380-6)

Schwarzacher, S. W., Smith, J. C. & Richter, D. W. 1995 Pre-Bötzinger complex in the cat. *J. Neurophysiol.* **73**, 1452–1461.

Smith, J. C., Ellenberger, H. H., Ballanyi, K., Richter, D. W. & Feldman, J. L. 1991 Pre-Botzinger complex: a brainstem region that may generate respiratory rhythm in mammals. *Science* **254**, 726–729. (doi:10.1126/science.1683005)

Tan, W., Janczewski, W. A., Yang, P., Shao, X. M., Callaway, E. M. & Feldman, J. L. 2008 Silencing pre-Bötzinger complex somatostatin-expressing neurons induces persistent apnea in awake rat. *Nat. Neurosci.* **11**, 538–540. (doi:10.1038/nn.2104)

Tanaka, I., Ezure, K. & Kondo, M. 2003 Distribution of glycine transporter 2 mRNA-containing neurons in relation to glutamic acid decarboxylase mRNA-containing neurons in rat medulla. *Neurosci. Res.* **47**, 139–151. (doi:10.1016/S0168-0102(03)00192-5)

Viemari, J. C. & Ramirez, J. M. 2006 Norepinephrine differentially modulates different types of respiratory pacemaker and nonpacemaker neurons. *J. Neurophysiol.* **95**, 2070–2082. (doi:10.1152/jn.01308.2005)

Wagner, E. J., Reyes-Vazquez, C., Ronnekleiv, O. K. & Kelly, M. J. 2000 The role of intrinsic and agonist-activated conductances in determining the firing patterns of preoptic area neurons in the guinea pig. *Brain Res.* **879**, 29–41. (doi:10.1016/S0006-8993(00)02698-6)

Winter, S. M., Fresemann, J., Schnell, C., Oku, Y., Hirrlinger, J. & Hülsmann, S. 2009 Glycinergic interneurons are functionally integrated into the inspiratory network of mouse medullary slices. *Pflugers Arch.* **24**, 459–469.